Transcriptome-proteome compendium of the Antarctic krill (*Euphausia superba*): Metabolic potential and repertoire of hydrolytic enzymes

Lars Möller[1] │ **Yeheven Vainstein[2]** │ **Lars Wöhlbrand[1]** │ **Marvin Dörries[1,5]** │ **Bettina Meyer [3,4,5]** │ **Kai Sohn[2]** │ **Ralf Rabus[1]**

[1] General and Molecular Microbiology, Institute for Chemistry and Biology of the Marine Environment (ICBM), Carl von Ossietzky University of Oldenburg, Oldenburg, Germany

[2] In-Vitro-Diagnostics, Fraunhofer Institute for Interfacial Engineering and Biotechnology (IGB), Stuttgart, Germany

[3] Biodiversity and Biological Processes in Polar Oceans, Institute for Chemistry and Biology of the Marine Environment (ICBM), Carl von Ossietzky University of Oldenburg, Oldenburg, Germany

[4] Ecophysiology of Pelagic Key Species, Alfred Wegener Institute, Helmholtz Centre for Polar and Marine Research, Bremerhaven, Germany

[5] Biodiversity Change, Helmholtz Institute for Functional Marine Biodiversity at the University of Oldenburg (HIFMB)**,** Oldenburg, Germany

Correspondence

Ralf Rabus, Institute for Chemistry and Biology of the Marine Environment (ICBM), Carl von Ossietzky University of Oldenburg, Carl-von-Ossietzky Str. 9-11, D-26111 Oldenburg, Germany.

Email: rabus@icbm.de

Abstract

The Antarctic krill (*Euphausia superba* Dana) is a keystone species in the Southern Ocean that uses an arsenal of hydrolases for biomacromolecule decomposition to effectively digest its omnivorous diet. The present study builds on a hybrid-assembled transcriptome (13,671 ORFs) combined with comprehensive proteome profiling. The analysis of individual krill compartments allowed detection of significantly more different proteins compared to that of the entire animal (1,464 *vs.* 294 proteins). The nearby krill sampling stations in the Bransfield Strait (Antarctic Peninsula) yielded rather uniform proteome datasets. Proteins related to energy production and lipid degradation were particularly abundant in the abdomen, agreeing with the high energy demand of muscle tissue. A total of 378 different biomacromolecule hydrolysing enzymes were detected, including 250 proteases, 99 CAZymes, 14 nucleases and 15 lipases. The large repertoire in proteases is in accord with the protein-rich diet affiliated with *E. superba*'s omnivorous lifestyle and complex biology. The richness in chitin-degrading enzymes allows not only digestion of zooplankton diet, but also the utilization of the discharged exoskeleton after moulting.

KEYWORDS

Antarctic krill, *Euphausia superba*, Bransfield Strait, hybrid assembly, transcriptomics, proteomics, krill compartments, functional categorisation, hydrolytic enzymes

Significance Statement

The Antarctic krill provides central ecosystems services to the Southern Ocean by grazing on autotroph and heterotroph diet and constituting the dominant food source for higher trophic levels. Moreover, *E. superba*'s broad repertoire of biomacromolecule hydrolysing enzymes represents a largely untapped resource for applied purposes. The transcriptome-proteome compendium of krill established in the present study provides a valuable basis for future studies on krill biology (e.g., metabolism, development, behaviour), for krill's contribution to organic matter turnover in the Southern Ocean, as well as for multilevel biotechnological prospecting.

1 │ INTRODUCTION

The Antarctic krill (*Euphausia superba* Dana, in the following called krill) is a keystone species in the Southern Ocean ecosystem by representing the key link between primary producers and higher trophic levels up to apex predators, such as penguins, seals, and whales [1]. Despite *E. superba*'s rather small body size of 6 cm and weight of 1 g, an estimated 8×10^{14} individuals account for a total biomass of 379 million tons [2]. The general lifestyle of *E. superba* as an omnivore is shifted towards herbivory in summer due to the then dominating phytoplankton blooms [3]. Food is taken up *via* a feeding basket, mechanically crushed in the gastric mill, and passed further into the digestive gland, where it is digested by an enzyme cocktail including proteases, cellulases/chitinases and laminarinases. The non-digested food is finally packed into fecal pellets in the hindgut and egested [3–5].

Next to the aforementioned ecosystem services, *E. superba* is also of major economic relevance. On the one hand, the krill fishery is the largest in the Southern Ocean in terms of tonnage caught. Krill is used as a diet additive for carnivorous fish in the aquaculture industry, as well as for human consumption and as source of high value fatty acids for the nutraceutical market [6, 7]. On the other hand, the unique set of biomacromolecule-decomposing hydrolases of *E. superba* are of increasing biotechnological interest due to advantages of cold-adapted enzymes [8] and catalytic specificities. For instance, proteases have been biochemically studied [9] and demonstrated to have medical application [10]. Furthermore, hydrolases breaking down the complex and diverse cell wall polysaccharides of algal food promise application in the biorefinery value-chain and the food industry [e.g., 11, 12].

Considerable insights into *E. superba*'s biology, ecology and physiology have already been gained [for overview see ref.13]. While its genome sequence has to date not been reported due to its large genome size of up to 48 Gbp [14], publicly available cDNA libraries have been sequenced to provide first insights into the encoded functions of krill [15–19]. By contrast, comprehensive proteomic analyses of *Euphausia* spp. are lacking, except for exploration of neuropeptides and peptidic hormones in the ice krill *Euphausia crystallorophis* [20].

The aim of the present study was to establish a comprehensive proteomic survey of *E. superba* by using dissected body compartments and to investigate main metabolic traits as well as the repertoire of hydrolytic enzymes. A transcriptome dataset of hybrid-assembled short- and long-read sequences was generated to enhance protein identification.

2 │ MATERIALS AND METHODS

2.1 │ Sample collection and krill dissection

Krill were caught on 11th June (Antarctic winter) during the AMLR Expedition 2016 with the research vessel Nathanie B. Palmer Cruise (NBP1606) at 3 different stations (I–III) within the Bransfield Strait (Figure 1); recorded physical and biological parameters are provided in Appendix S1. Krill was caught with an Isaak Kit Midwater Trawl net towed from 170 m depth to the surface. Freshly caught krill was immediately shock-frozen in liquid N_2 and stored at –80°C until further processing.

For proteomic and transcriptomic analyses, only adult females stage B2 were used for better comparability. In total, 15 krill individuals from all stations were dissected on ice into head, carapace, abdomen and telson (Figure 2); eyes, reproduction organs and intestines were discarded. Compartmentalization was based on proposed main functionalities of the body parts: head, harbouring most of sensory functions and high activity of circadian clock; carapace, representing a triglyceride storage; abdomen, consisting mainly of muscle proteins; and telson, a construct mainly formed of muscle and chitin. Following dissection, compartments were immediately shock-frozen in liquid N_2 and stored at –80°C until further processing. Additional proteomic analyses were done on three non-dissected entire animals caught at station I.

2.2 │ RNA isolation

RNA from dissected compartments was isolated using the RNeasy Plus Mini Kit and QiaCube (both Qiagen, Hilden, Germany). Frozen tissue was disrupted with a Retsch vibrating mill (Model MM200; Retsch GmbH, Haan, Germany) at 30 Hz shaking frequency for 2 min and then processed as described according to the manufacturer's instructions. RNA content was quantified using the Qubit RNA HS Assay Kit (Life Technologies, Carlsbad, CA, USA) and quality controlled with the HS RNA Analysis Kit on the Fragment Analyzer (Advanced Analytical, Ankeny, IA, USA).

2.3 │ cDNA sequencing

For long reads, the cDNA kit SQK-DCS109 (Oxford Nanopore Technologies Ltd., Oxford, UK) was used, allowing sequencing without prior PCR amplification. 25 ng of total RNA from each krill compartment were pooled yielding a total of 100 ng, prepared with SQK-DCS109 kit and loaded on Spoton Flow Cells MkI R9.4. The sequencing was performed with a MinION instrument (Oxford Nanopore Technologies Ltd.) for 48 h using MinKnow, followed by base-calling with Guppy using default settings, resulting in 727,000 reads. Adapter sequences were removed using Porechop and remaining reads trimmed using NanoFilt to ensure a minimal read length of 50 bp. The Phred score threshold was set above 7. The quality of the raw reads and trimmed reads was controlled with NanoPlot. The remaining 616,000 trimmed sequences showed a mean quality score of 9.7.

For short reads, libraries were prepared separately for each krill compartment using the Illumina TruSeq stranded mRNA Kit (Illumina, San Diego, CA, USA) and the standard protocol on a Biomek FXP pipetting robot (Beckman Coulter, Brea, CA, USA), applying the recommended amount of 200 ng of RNA. Sequencing was performed on a HiSeq2500 instrument (Illumina) *via* Rapid Run in a paired-end mode with 2×100 cycles for every sample, resulting in an average sequence depth of $\sim 22 \times 10^6$ reads per sample with an average >Q30 of 95%. Sequence processing was performed by de-multiplexing using bcl2fastq-1.8.4 (Illumina). Parameters were set on default for adapter trimming with a threshold of 90% base match and no mismatches allowed in sequencing barcode. Then, remaining reads were quality-based trimmed to remove potential contaminants, low quality reads and sequencing adapters with the help of BBDuk. Quality thresholds were set on at least 20 for Phred and a minimal read length after quality-based and adapter trimming of 50 bp. Additionally, every sample was manually inspected and quality-controlled before and after trimming with FastQC. Per base sequence quality, average base composition, GC content, sequence length distribution and adapter contaminations were checked after trimming.

References for applied software (including used version) are provided in Appendix S2.

2.4 │ Sequence assembly and quality control

Quality and adapter trimmed sequences from the 4 dissected krill compartments were merged to a single dataset and interleaved sets were generated with "ngm-utils interleave" from NextGenMap. In order to reduce read redundancy and decrease sampling variations from merging, digital normalization was applied with khmer using default settings of ksize 32 and cutoff 20.

Remaining normalized, quality- and adapter-trimmed sequences from Nanopore and Illumina sequencing were assembled by a SPAdes assembler in rna mode (k: 33,55,67,77, pe: 1−12, minimal-contig length of 150 bp). Then, contigs with a coverage below 10 were

removed using custom Perl script fastA_filter_contigs.pl, resulting in 36,932 contigs with a total of 24.9 Mbp and an average length of 216 bp.

Completeness of the assembled transcriptome using the ORFs content was evaluated by BUSCO and comprised 50.83%. Additionally, the assembly statistics and quality were analyzed by rnaQUAST.

For draft transcriptome polishing, base accuracy of assembled contigs was improved by two-step polishing for raw long reads and a single polishing step with short reads. Trimmed long reads were mapped to a draft assembly using minimap2 and the resulting SAM file was sorted and indexed using Samtools. The index SAM file together with the raw long reads in Fast5 format were used to polish a draft assembly by NanoPolish. The newly generated improved draft assembly, was polished with Pilon in two iterations using short reads. Default settings were used, introducing base corrections, fixing mis-assemblies and filling gaps in the transcriptome assembly. Each time, the resulting draft of the multi-step polishing pipeline was used as an input for the next iteration of assembly polishing.

The workflow of the hybrid assembly is detailed in Appendix S3 and references for applied software (including used version) in Appendix S2.

2.5 │ ORF prediction and annotation

Assembled and quality improved contigs were translated to coding protein sequences using TransDecoder with default settings, resulting in predicted proteins with lengths between 86 and 2,370 amino acids. The remaining ORFs were annotated *via* three steps: (i) initial annotation with Protein-Protein BLAST using Swiss-Prot Uniref90 database as a reference; (ii) protein family prediction with hmmscan by searching the Pfam database using profile hidden Markov models; and (iii) final annotation with InterProScan including an additionally activated search for GO terms and pathways.

The fully annotated krill transcriptome dataset, which was generated *via* the hybrid assembly approach, comprises 13,671 ORFs, cumulatively amounting to 13.44 Mbp. Among them, 11,228 ORFs have a matching UniRef90 number, 6,554 an associated InterPro annotation, and 11,064 a matching Pfam protein family.

References for applied software (including used version) are provided in Appendix S2.

2.6 │ Proteomic analyses

For proteomic analyses, 5 individual animals per sampling station were dissected into the 4 compartments (outlined above, section 2.1). Furthermore, 3 non-dissected individuals (station I) were analysed and processed. Complete krill samples and dissected compartments were directly transferred into 2-mL screwcap vials containing ceramic beads (1.4 and 2.8 mm diameter; Precellys, Montigny Le Bretonneux, France). Following addition of 400 μL lysis buffer (7 M urea, 2 M thiourea, 30 mM Tris/HCl, pH 8.5) for head and telson, or 1,000 μL for carapace and abdomen, each sample was subjected to bead beating at a speed of 10 m/s for 15 s (FastPrep-24 5G; MP Biomedical, Schwerte, Germany) and 300 s incubation on ice with 3 repetitions. Debris was removed by centrifugation (20,000 × g, 10 min, 4°C) and protein content of supernatants determined according to the method described by Bradford [21] using BSA as standard. Then, 10 μg total protein per sample (specific compartment of each individual krill as well as whole protein extract of krill from station I) were applied to SDS-PAGE separation using mini gels (12.5% acrylamide, 0.75 mm thickness) and postelectrophoretically stained with Coomassie Brilliant Blue [22]. Each sample lane was cut into 8 slices, and each slice into small pieces (~1 mm^3) prior to washing, reduction, alkylation and tryptic digest [23]. Generated peptides were separated using a nanoLC system (nanoRSLC; ThermoFisher Scientific, Germering, Bavaria, Germany) operated in trap-column mode (2 cm, 75 μm inner diameter, 5 μm bead size; ThermoFisher Scientific), equipped with a 25-cm separation column (75 μm inner diameter, 2 μm bead size; ThermoFisher Scientific) and applying a 130-min linear gradient of increasing acetonitrile concentration [24]. The eluent was continuously ionized (captive spray ion source; Bruker Daltonik GmbH, Bremen, Germany) and analysed by an ion trap (amaZon speed ETD; Bruker Daltonik GmbH). The instrument was operated in positive mode with a capillary current of 1.3 kV and drygas flow of 3 L/min at 150°C. Active precursor exclusion was set for 0.2 min. Per full scan MS, 20 MS/MS spectra of the most intense masses were acquired. Protein identification was performed against the translated transcriptome using Mascot (v. 2.3; Matrix Science Ltd., London, UK) *via* the ProteinScape platform (v. 4.2; Bruker Daltonik GmbH) applying a mass tolerance of 0.3 Da for MS and 0.4 Da for MS/MS searches and a target decoy strategy (false discovery rate <1%). Search results for each sample slice were compiled using the protein extractor of ProteinScape. Protein identification data are compiled in Appendix S4.

2.7 │ Multivariate and statistical analyses of proteome dataset

For comparison of compartment sub-proteomes and overall krill proteome, a non-metric multidimensional scaling (nMDS) based on a Bray-Curtis-Dissimilarity was applied. The nMDS plot was created with vegan and ggplot 2. The ordination yielding low stress values was based on 1,000 attempts and compartments were visualized in groups by a 95% confidence interval in the nMDS-ordination. The nMDS-plot was tested for significant

differences between the visual compartments by PERMANOVA. Additionally, PERMDISP-routine was used to test for significance from dispersion effects with funfuns.

The absolute number of unique detected proteins in the proteome datasets of the compartments as well as the short-read transcriptome datasets were used for Venn-diagramm analyses. Visualization was done with the program R and the package VennDiagramm.

References for applied software (including used version) are provided in Appendix S2.

2.8 │ Hydrolase and CAZyme identification

For the prediction of potential hydrolases and CAZymes, annotated proteins from the hybrid assembly were screened for predictable properties indicating respective functions. EC-numbers, InterPro-domains and GO-groups correlated to CAZymes, lipases, nucleases and proteases (Appendix S5) were used and checked against the annotated hybrid-assembled transcriptome. In addition, SwissProt-entries with defined or predicted biochemical functions were used to tentatively assign target molecules/bonds to the predicted hydrolases. Afterwards, the presence of potential hydrolysing enzymes was searched for in the sub-proteomes of compartments and short-read transcriptome datasets. Visualization of the results was done by R with package ggplot2.

8

3 │ RESULTS AND DISCUSSION

3.1 │ Transcriptome and proteome datasets

The workflow for generating and integrating the transcriptome and proteome datasets is schemed in Figure 2. A comprehensive transcriptome dataset was generated from one female individual krill (station I). This involved short-read sequencing per compartment (each ~22×10^6 reads) and long-read sequencing of the combined compartments (616,000 reads). The subsequent hybrid assembly yielded 13,671 predicted ORFs with an improved gene coverage benefitting subsequent protein identification. These ORFs were subjected to automated protein prediction and functional assignment.

Using the predicted ORFs of the hybrid-assembled krill transcriptome, a total of 1,475 different proteins could be identified, covering ~10% of the predicted proteins. Such deviations between transcriptome and proteome datasets typically reflect the dynamic linkage between these two consecutive steps of genetic information processing [25]. Furthermore, the high dynamic range between cellular proteins (up to 10^{12}) [26–28] causes overrepresentation of highly abundant proteins. Such "shadowing" effects are far less pronounced (10^3–10^4) with mRNA [29] and the sheer number of sequence reads increases the probability of detecting low abundant mRNAs.

However, it should be considered that probability-based protein identification depends on the representativeness of the underlying protein database. Regarding protein size distribution, the transcriptome-based ORF-set revealed a shift towards smaller proteins (median 22 kDa) (Figure 3A) as compared to other crustaceans (median 23–46 kDa) such as inferred from short-read sequencing-based genomes of *Daphnia magna* (big water flea; acc. no., GCA_001632505), *Dp. pulex* (common water flea; acc. no., GCA_000187875), and *Penaeus vannamei* (white shrimp; acc. no., GCA_003789085), and mRNA-based predicted proteome of *Carcinus maenas* (common beach crab; AniProtDB [30]). Hence, larger sized proteins are most likely underrepresented in the used ORF-set. In consequence, detected peptides corresponding to larger proteins not represented in the transcriptome-derived ORF-set could not be allocated to these proteins, yielding a lower number of identifiable proteins.

3.2 │ Benefit of proteomic analysis per krill compartment

The analyses of the different proteome datasets using nMDS revealed rather distinct grouping per compartment with abdomen and telson being the most similar, and head and carapace more distantly related (Figure 3B). However, within a given compartment, the

proteome pattern was very similar across sampling stations I–III. Krill sampling was performed in close succession between stations, with high food availability in terms of chlorophyll *a* concentration (4.2 and 6.4 mg/m^3) and similar sea surface temperature (-1.7 and $1.8°C$), implicating rather congruent physiological conditions.

GeLC MS-based analyses of dissected compartments yielded detection of 692–894 different proteins (Figure 3C). In contrast, applying the same approach on non-dissected animals resulted in only a total of 294 different proteins (not shown). However, the number of detected peptides was comparable between all sample types. Apparently, the abundant proteins (and their peptides) of the different compartments are overrepresented in the entire animal samples, since >92% of the 294 most abundant proteins of the compartment samples are covered by the proteins detected in the entire animal samples (even >82% of the top 200). Hence, pre-analysis decomplexation by dissecting compartments is very beneficial for in depth proteomic analyses of krill. Analyses of the dissected animals revealed 135–196 apparently compartment-specific proteins and 331 proteins that are shared between compartments.

In contrast to these proteomic data, the short-read transcriptome data revealed no distinct profiles with the vast majority of transcripts detected in all 4 compartments (88.3%; Figure 3D). This is most likely due to a higher sensitivity and yield of the transcriptomic approach ($\sim22 \times 10^6$ reads per compartment). Hence, also low abundant transcripts may be detected while the corresponding low abundant proteins may not. These findings are in accord with a previous study on *E. superba*, where cDNA libraries were prepared each for head, abdomen, photophores and thoracopods, yielding only one potential tissue-specific mRNA for a myosin light chain amongst more than 1,000 different mRNAs in the abdomen [31].

3.3 │ Functional categorisation of krill compartment proteomes

The annotation of the identified 1,475 proteins was manually refined and the allocation to superior functional categories per analysed compartment is summarized in Figure 4. The largest numbers of detected proteins belong to cellular structures, signalling & regulation and transport, together comprising $\sim40\%$ of detected proteins per compartment. The high abundances of cellular structure proteins (20–25%), are mainly explained by the detection of actin and myosin, which alone account for 10% of the overall detected proteins. Actin, as one of the most abundant intracellular proteins in eukaryotes can account for 10–15% of the overall cellular protein content [32–34], and myosin up to 18% of total cell mass in muscle cells [35].

Striking differences in proteome composition were observed for the categories of energy production and lipid degradation, having almost 3-fold higher abundances in krill

abdomen compared to the other three compartments. As an example, the energy production category includes 15 copies of arginine kinases. This enzyme serves in crustaceans a similar function as creatine kinases in high energy depending tissue of mammals (e.g., heart and claw muscle) for maintenance of intracellular ATP [36–39]. Since lipid degradation proteins are also overrepresented in the krill muscle, it can be hypothesized that energy is mainly generated from lipid catabolism in this compartment. Accordingly, lipase activity in *E. superba* was reported to be 4-fold higher in abdominal muscle and to represent a 15-fold higher share of total esterase activity compared to the whole animal [40]. Furthermore, lipids are well-documented as important energy reserve for crustaceans [41, 42], in particular during periods of starvation or adaptation [43, 44]. Since important storage reserves are localized in heptopancrease and the muscles, it suggests itself that enzymes for their mobilization are produced in the same tissues [45].

Proteins of the immune and haemolymphe systems are ~1.5-fold more abundant in the carapace, agreeing with this compartment harbouring heart, as well as other main parts of the haemolymph system in crustaceans like shrimp and krill [34]. This group of proteins comprises the copper-containing oxygen transporter haemocyanin as well as proteins of the immune response like lectin and clotting proteins [46–49].

3.4 │ Hydrolase repertoire across krill compartments

E. superba has a multifaceted feeding behaviour ranging from ice algae, filter feeding of small copepods and phytoplankton, extraction of benthic phytodetrius to possibly even raptorial feeding on larger copepods [3, 50–52]. Since this nutritional diversity requires a broad array of digestive enzymes for efficient nutrient usage, this study put an emphasis also on the enzymatic potential for hydrolysing biomacromolecules. In total, 733 candidates (Figure 5, Table 1) were detected by targeted search in the transcriptome-proteome compendium, accounting for 5% of the complete transcriptome dataset. According to predicted substrate specificity, these candidates include 483 proteases, 179 CAZymes, 38 lipases and 33 nucleases, covering a broad range of potential target molecules/bonds as inferred from homologous SwissProt-entries: 69, 23, 10, and 8, respectively (Table 1). About half of these enzymes could be detected in the transcriptome or proteome datasets per compartment. The hydrolases detected in the proteome covered approx. 10% of the enzymes predicted from the hybrid-assembled krill transcriptome, agreeing with the ratio observed for the complete protein dataset. Furthermore, in general at least four times more hydrolases were detected by transcriptomics as compared to proteomics. Since transcriptome and proteome are dynamically linked one might consider that the hydrolases found in the transcriptome reveal the range of those potentially deployable by the Antarctic krill [25]. On the other hand, those detected in the proteome probably better represent the effectively used hydrolases. Furthermore, this discrepancy in numbers of hydrolases

11

detectable by the two applied OMICS approaches is very likely enhanced by their different analytical sensitivities [26-29].

The high share of proteases detected in the present study agrees with previous reports, which link the high efficiency of food usage in Antarctic krill to its high proteolytic enzyme activity [9]. The group of peptidases comprises diverse endo- and exopeptidases with a broad spectrum of specificities and hydrolysing profiles. This includes candidates already described as digestive enzymes of *E. superba* and other crustaceans, e.g., cathepsins [53–56], chymotrypsin [57–59], and trypsin [9, 59]. Crustaceans and *E. superba* produce digestive enzymes (including peptidases) mainly in the hepatopancreas or hind gut, but also in other body parts like the abdominal muscle of krill [5, 53]. Moreover, multiple detected proteases serve cellular functions in signal cascades and production of molecular cues (e.g., immune response, blood coagulation and hormones).

Previously reported polysaccharide hydrolysing enzymes of krill include amylases, laminarinases, cellulases and chitinases [5, 60], some of which have also been detected in the present study. Chitin-degrading enzymes represent a major fraction of the here detected CAZymes of krill, including chitinases (breaking chitin backbone), chitooligosaccharolytic-acetylglucosaminidases (acting on oligomeric breakdown products of chitin) and deacetylases (removing the acetyl-group from monomers). These broad chitin-degrading capacities agree well with *E. superba*'s capability to feed on copepods. Furthermore, these enzymes are likely required during moulting (like in other crustaceans) and could even be used to utilize the discharged chitin exoskeleton [3, 51, 61, 62].

The Antarctic krill stores lipids in the form of triacylglycerols [63] and crustaceans use muscles, hepatopancreas and ovaries as storage places. Triacylglycerols are degraded by initial cleavage of fatty acid sidechains from the glycerol backbone by "true lipases" (triacylglyceroyl hydrolases). These enzymes are known to be present in the krill muscle [40] and were also found in the present transcriptome dataset. Further detected lipases included phospholipases, sphingomyelin phosphodiesterases and carboxylesterases, which might play important roles in the metabolism of structural lipids.

Nucleases have also been reported to be produced in the digestive gland of Antarctic krill, besides lipases, CAZymes and peptidases [64], and related to decomposition of food [10]. In the present study, several nucleases targeting RNA or DNA were detected, but a clear assignment to digestive functions remains unclear at present, due to their fundamental molecular functions in the cell.

4 | CONCLUSIONS AND OUTLOOK

The presented transcriptome-proteome compendium of *E. superba* combines a high-quality hybrid-assembled transcriptome with a comprehensive proteomic profiling of dissected body

compartments. It provides functional insights into the general metabolic potential and enzymatic arsenal employed by the omnivore *E. superba* during Antarctic winter. This compendium and assessment of the compartment-specific proteomic approach will benefit future studies on this keystone species of the Southern Oceans with respect to a wide range of research topics ranging from fundamental studies to the biotechnological prospecting of biomacromolecule hydrolyzing enzymes. Moreover, this compendium provides a valuable resource to differentiate such krill enzymes from those of its microbiome. Considering that the digestive tract of an average-sized krill has an estimated volume of 100 μL, a summertime peak population comprises a combined volume of 8×10^{10} L (8×10^7 m^3). This represents an enormous reaction space for the turnover of complex organic matter and therefore a promising and largely untapped reservoir of biotechnological exploitation for hydrolytic enzymes.

CONFLICT OF INTEREST

There are no conflicts of interests.

DATA AVAILABILITY STATEMENT

Transcriptomic data were deposited at NCBI as BioProject PRJNA787908. The mass spectrometry proteomics data have been deposited to the ProteomeXchange Consortium *via* the PRIDE [65] partner repository with the dataset identifiers PXD033594 (carapace), PXD033597 (head), PXD033601 (muscle), PXD033602 (whole body), and PXD033775 (telson). Furthermore, proteomic data are compiled in Appendix 4.

ORCID

Ralf Rabus https://orcid.org/0000-0001-5536-431X

Lars Wöhlbrand https://orcid.org/0000-0001-7253-3373

Bettina Meyer https://orcid.org/0000-0001-6804-9896

APPENDIX

S1. Parameters of sampling sites.

S2. References of employed bioinformatic software tools.

S3. Workflow of hybrid assembly.

S4. Protein identification data.

S5. GO-terms etc. of studied hydrolases.

REFERENCES

1. Murphy, E.J., Watkins, J.L., Trathan, P.N., Reid, K., Meredith, M.P., Thorpe, S.E., … Fleming, A.H. (2007). Spatial and temporal operation of the Scotia Sea ecosystem: a review of large-scale links in a krill centred food web. *Philosophical Transactions of the Royal Society B*, *362*(1477), 113–148.

2. Atkinson, A., Siegel, V., Pakhomov, E.A., Jessopp, M.J., & Loeb, V. (2009). A re-appraisal of the total biomass and annual production of Antarctic krill. *Deep-Sea Research I*, *56*(5), 727–740.

3. Schmidt, K., & Atkinson, A. (2016). Feeding and food processing in Antarctic krill (*Euphausia superba* Dana). In. Siegel, V. (ed.), Biology and ecology of Antarctic krill, Advances in polar ecology. chp. 5, 175–224.

4. Buchholz, F., & Saborowski, R. (1996). A field study on the physiology of digestion in the Antarctic krill, *Euphausia superba*, with special regard to chitinolytic enzymes. *Journal of Plankton Research*, *18*(6), 895–906.

5. Saborowski, R., & Buchholz, F. (1999). A laboratory study on digestive processes in the Antarctic krill, *Euphausia superba*, with special regard to chitinolytic enzymes. *Polar Biology*, *21*(5), 295–304.

6. Albalat, A., Nadler, L.E., Foo, N., Dick, J.R., Watts, A.J.R., Philp, H., … Monroig, O. (2016). Lipid composition of oil extracted from wasted Norway lobster (*Nephrops norvegicus*) heads and comparison with oil extracted from Antarctic krill (*Euphasia superba*). *Marine Drugs*, *14*(12), 219.

7. Grant, S.M., Hill, S.L., Trathan, P.N., & Murphy, E.J. (2013). Ecosystem services of the Southern Ocean: trade-offs in decision-making. *Antarctic Science*, *25*(5), 603–617.

8. Duarte, A.W.F., dos Santos, J.A., Vianna, M.V., Vieira, J.M.F., Mallagutti, V.H., Inforsato, F.J., … Sette, L.D. (2018). Cold-adapted enzymes produced by fungi from terrestrial and marine Antarctic environments. *Critical Reviews in Biotechnology*, *38*(4), 600–619.

9. Sjödahl, J., Emmer, Å., Vincent, J., & Roeraade, J. (2002). Characterization or proteinases from Antarctic krill (*Euphausia superba*). *Protein Expression and Purification*, *26*(1), 153–161.

10. Hellgren, L., Karlstam, B., Mohr, V., & Vincent, J. (1999). Peptide hydrolases from antarctic krill – an important new tool with a promising medical potential. In: Margesin, R., & Schinner, F. (eds), Biotechnological applications of cold-adapted organisms. Springer-Verlag, Berlin, p. 63–74.

11. Balabanova, L., Slepchenko, L., Son, O., & Tekutyeva, L. (2018). Biotechnology potential of marine fungi degrading plant and algae polymeric substrates. *Frontiers in Microbiology*, *9*, 1527.

12. Trincone, A. (2018). Update on marine carbohydrate hydrolyzing enzymes: biotechnological applications. *Molecules*, *23*(4), 901.

13. Meyer, B. (2012). The overwintering of Antarctic krill, *Euphausia superba*, from an ecophysiological perspective. *Polar Biology*, *35*(1), 15–37.

14. Jeffery, N.W. (2012). The first genome size estimates for six species of krill (Malacostraca, Euphausiidae): large genomes at the north and south poles. *Polar Biology*, *35*(6), 959–962.

15. Hunt, B.J., Özkaya, Ö., Davies, N.J., Gaten, E., Seear, P., Kyriacou, C.P., Tarling, G., & Rosato, E. (2017). The *Euphausia superba* transcriptome database, SuperbaSE: an online, open resource for researchers. *Ecology and Evolution*, *7*(16), 6060–6077.

16. Ma, C., Ma, H., Xu, G., Feng, C., Ma, L., & Wang, L. (2018). *De novo* sequencing of the Antarctic krill (*Euphausia superba*) transcriptome to identify functional genes and molecular markers. *Journal of Genetics*, *97*(4), 995–999.

17. Martins, M.J.F., Lago-Leston, A., Anjos, A., Duarte, C.M., Agusti, S., Serrão, E.A., & Pearson, G.A. (2015). A transcriptome resource of Antarctic krill (*Euphausia superba* Dana) exposed to short-term stress. *Marine Genomics*, *23*, 45–47.

18. Meyer, B., Martini, P., Biscontin, A., de Pittá, C., Romualdi, C., Teschke, M., … Kawaguchi, S. (2015). Pyrosequencing and *de novo* assembly of Antarctic krill (*Euphausia superba*) transcriptome to study the adaptability of krill to climate-induced environmental changes. *Molecular Ecology Resources*, *15*(6), 1460–1471.

19. Sales, G., Deagle, B.E., Calura, E., Martini, P., Biscontin, A., de Pittá, C., … Jarman, S. (2017). KrillDB: A *de novo* transcriptome database for the Antarctic krill (*Euphausia superba*). *PLoS ONE*, *12*(2), e0171908.

Accepted Article

20. Toullec, J.-Y., Corre, E., Bernay, B., Thorne, M.A.S., Cascella, K., Ollivaux, C., … Clark, M.S. (2013). Transcriptome and peptidome characterisation of the main neuropeptides and peptidic hormones of a Euphausiid: the ice krill, *Euphausia crystallorophias*. *PLoS ONE*, *8*(8), e71609.

21. Bradford, M.M. (1976). A rapid and sensitive method for the quantitation of microgram quantities of protein utilizing the principle of protein-dye binding. *Analytical Biochemistry*, *72*(1–2), 248–254.

22. Neuhoff, V., Arold, N., Taube, D., & Ehrhardt, W. (1988). Improved staining of proteins in polyacrylamide gels including isoelectric focusing gels with clear background at nanogram sensitivity using Coomassie Brilliant Blue G-250 and R-250. *Electrophoresis*, *9*(6), 255–262.

23. Koßmehl, S., Wöhlbrand, L., Drüppel, K., Feenders, C., Blasius, B., & Rabus, R. (2013). Subcellular protein localization (cell envelope) in *Phaeobacter inhibens* DSM 17395. *Proteomics*, *13*(18–19), 2743–2760.

24. Wöhlbrand, L., Rabus, R., Blasius, B., & Feenders, C. (2017). Influence of nanoLC column and gradient length as well as MS/MS frequency and sample complexity on shotgun protein identification of marine bacteria. *Journal of Molecular Microbiology and Biotechnology*, *27*(3), 199–212.

25. Tuli, L., & Ressom, H.W. (2009). LC–MS based detection of differential protein expression. *Journal of Proteomics and Bioinformatics*, *2*(10), 416–438.

26. Anderson, N.L., & Anderson, N.G. (2002). The human plasma proteome. History, character, and diagnostic prospects. *Molecular & Cellular Proteomics*, *1*(11), 845–867.

27. Fonslow, B.R., Carvalho, P.C., Academia, K., Freeby, S., Xu, T., Nakorchevsky, A., … Yates III, J.R. (2011). Improvements in proteomic metrics of low abundance proteins through proteome equalization using ProteoMiner prior to MudPIT. *Journal of Proteome Research*, *10*(8), 3690–3700.

28. Beck, M., Claassen, M., & Aebersold, R. (2011). Comprehensive proteomics. *Current Opinion in Biotechnology*, *22*(1), 3–8.

29. Marinov, G.K., Williams, B.A., McCue, K., Schroth, G.P., Gertz, J., Myers, R.M., & Wold, B.J. (2014). From single-cell to cell-pool transcriptomes: stochasticity in gene expression and RNA splicing. *Genome Research*, *24*(3), 496–510.

30. Barreira, S.N., Nguyen, A.-D., Fredriksen, M.T., Wolfsberg, T.G., Moreland, R.T., & Baxevanis, A.D. (2021). AniProtDB: a collection of consistently generated metazoan proteomes for comparative genomics studies. *Molecular Biology and Evolution*, *38*(10), 4628–4633.

31. de Pittá, C., Bertolucci, C., Mazzotta, G.M., Bernante, F., Rizzo, G., de Nardi, B., Pallavicini, A., Lanfranchi, G., & Costa, R. (2008). Systematic sequencing of mRNA from Antarctic krill *(Euphausia superba)* and first tissue specific transcriptional signature. *BMC Genomics*, *9*, 45.

32. Bray, D., & Thomas, C. (1975). The actin content of fibroblasts. *Biochemical Journal*, *147*(2), 221–228.

33. Egelman, E.H. (2012). Chp. 4.3 Structure and dynamic states of actin filaments. In: Egelman (ed), Comprehensive Biophysics, Elsevier, Amsterdam, *4*, 15–30.

34. Göpel, T., & Wirkner, C.S. (2020). The circulatory system of *Penaeus vannamei* Boone, 1931–Lacunar function and a reconsideration of the "open vs. closed system" debate. *Journal of Morphology*, *281*(4–5), 500–512.

35. Deshmukh, A.S., Murgia, M., Nagaraj, N., Treebak, J.T., Cox, J., & Mann, M. (2015). Deep proteomics of mouse skeletal muscle enables quantitation of protein isoforms, metabolic pathways, and transcription factors. *Molecular & Cellular Proteomics*, *14*(4), 841–853.

36. Wallimann, T., Wyss, M., Brdiczka, D., Nicolay, K., & Eppenberger, H.M. (1992). Intracellular compartmentation, structure and function of creatine kinase isoenzymes in tissues with high and fluctuating energy demands: the 'phosphocreatine circuit' for cellular energy homeostasis. *Biochemical Journal*, *281*(1), 21–40.

37. France, R.M., Sellers, D.S., & Grossmann, S.H. (1997). Purification, characterization, and hydrodynamic properties of arginine kinase from Gulf shrimp (*Penaeus aztecus*). *Archives of Biochemistry and Biophysics*, *345*(1), 73–78.

38. Kotlyar, S., Weihrauch, D., Paulsen, R.S., & Towle, D.W. (2000). Expression of arginine kinase enzymatic activity and mRNA in gills of the euryhaline crabs *Carcinus maenas* and *Callinectes sapidus*. *The Journal of Experimental Biology*, *203*(16), 2395–2404.

39. Kang, L., Shi, H., Liu, X., Zhang, C., Yao, Q., Wang, Y., … Chen, K. (2011). Arginine kinase is highly expressed in a resistant strain of silkworm (*Bombyx mori*, Lepidoptera): implication of its role in resistance to *Bombyx mori* nucleopolyhedrovirus. *Comparative Biochemistry and Physiology Part B*, *158*(3), 230–234.

40. Auerswald, L., Meyer, B., Teschke, M., Hagen, W., & Kawaguchi, S. (2015). Physiological response of adult Antarctic krill, *Euphausia superba*, to long-term starvation. *Polar Biology*, *38*(6), 763–780.

41. Macedo, C.F., & Pinto-Coelho, R.M. (2001). Nutritional status response of *Daphnia laevis* and *Moina micrura* from a tropical reservoir to different algal diets: *Scenedesmus quadricauda* and *Ankistrodesmus gracilis*. *Brazilian Journal of Biology*, *61*(4), 555–562.

42. Mika, A., Skorkowski, E., Stepnowski, P., & Gołębiowski, M. (2013). Identification of lipid components in the abdominal muscle of fall-caught *Crangon crangon* from a coastal area of the Baltic Sea. *Journal of the Brazilian Chemical Society*, *24*(3), 439–448.

43. Barclay, M.C., Dall, W., & Smith, D.M. (1983). Changes in lipid and protein during starvation and moulting cycle in the tiger prawn, *Penaeus esculentus* Haswell. *Journal of Experimental Marine Biology and Ecology*, *68*(3), 229–244.

44. Luvizotto-Santos, R., Lee, J.T., Branco, Z.P., Bianchini, A., & Nery, L.E.M. (2003). Lipids as energy source during salinity acclimation in the euryhaline crab *Chasmagnathus granulata* Dana, 1851 (Crustacea-Grapsidae). *Journal of Experimental Zoology*, *295A*(2), 200–205.

45. Sánchez-Paz, A., García-Carreño, F., Muhlia-Almazán, A., Peregrino-Uriarte, A.B., Hernández-López, J., & Yepiz-Plascencia, G. (2006). Usage of energy reserves in crustaceans during starvation: status and future directions. *Insect Biochemistry and Molecular Biology*, *36*(4), 241–249.

46. Cahill Jr., G.F. (1976). Starvation in man. *Clinics in Endocrinology and Metabolism*, *5*(2), 397–415.

47. Gaykema, W.P.J., Hol, W.G.J., Vereijken, J.M., Soeter, N.M., Bak, H.J., & Beintema, J.J. (1984). 3.2 Å structure of the copper-containing, oxygen-carrying protein *Panulirus interruptus* haemocyanin. *Nature*, *309*(5963), 23–29.

48. Wang, X.-W., Xu, J.-D., Zhao, X.-F., Vasta, G.R., & Wang, J.-X. (2014). A shrimp C-type lectin inhibits proliferation of the hemolymph microbiota by maintaining the expression of antimicrobial peptides. *The Journal of Biological Chemistry*, *289*(17), 11779–11790.

49. Wang, J., Janech, M.G., & Burnett, K.G. (2019). Protein-level evidence of novel β-type hemocyanin and heterogeneous subunit usage in the Pacific whiteleg shrimp, *Litopenaeus vannamei*. *Frontiers in Marine Sciences*, *6*, 687.

50. Hamner, W.M. (1988). Biomechanics of filter feeding in the Antarctic krill *Euphausia superba*: review of past work and new observations. *Journal of Crustacean Biology*, *8*(2), 149–163.

51. Hopkins, T.L., & Torres, J.J. (1989). Midwater food web in the vicinity of a marginal ice zone in the western Weddell Sea. *Deep-Sea Research*, *36*(4), 543–560.

52. Clarke, A., & Tyler, P.A. (2008). Adult Antarctic krill feeding at abyssal depths. *Current Biology*, *18*(4), 282–285.

53. Kimoto, K., Fukamizu, A., & Murakami, K. (1986). Partial purification and characterization of proteinases from abdomen part muscle of Antarctic krill. *Bulletin of the Japanese Society of Scientific Fisheries*, *52*(4), 745–749.

54. Denys, C.J., & Brown, P.K. (1982). Euphausiid visual pigments. The rhodopsins of *Euphausia superba* and *Meganyctiphanes norvegica* (*Crustacea*, *Euphausiacea*). *Journal of General Physiology*, *80*(3), 451–472.

55. Hu, K.-J., & Leung, P.-C. (2007). Food digestion by cathepsin L and digestion-related rapid cell differentiation in shrimp hepatopancreas. *Comparative Biochemistry and Physiology Part B*, *146*(1), 69–80.

56. Rojo, L., Muhlia-Almazan, A., Saborowski, R., & García-Carreño, F. (2010). Aspartic cathepsin D endopeptidase contributes to extracellular digestion in clawed lobsters *Homarus americanus* and *Homarus gammarus*. *Marine Biotechnology*, *12*(6), 696–707.

57. Kimoto, K., Yokoi, T., & Murakami, K. (1985). Purification and characterization of chymotrypsin-like proteinase from *Euphausia superba*. *Agricultural and Biological Chemistry*, *49*(6), 1599–1603.

58. Hernández-Cortés, P., Whitaker, J.R., & García-Carreño, F.L. (1997). Purification and characterization of chymotrypsin from *Penaeus vannamei* (*Crustacea*: Decapoda). *Journal of Food Biochemistry*, *21*(1), 497–514.

59. von Elert, E., Agrawal, M.K., Gebauer, C., Jaensch, H., Bauer, U., & Zitt, A. (2004). Protease activity in gut of *Daphnia magna*: evidence for trypsin and chymotrypsin enzymes. *Comparative Biochemistry and Physiology Part B*, *137*(3), 287–296.

60. Meyer, B., Saborowski, R., Atkinson, A., Buchholz, F., & Bathmann, U. (2002). Seasonal differences in citrate synthase and digestive enzyme activity in larval and postlarval Antarctic krill, *Euphausia superba*. *Marine Biology*, *141*(5), 855–862.

61. Schmidt, K., Atkinson, A., Pond, D.W., & Ireland, L.C. (2014). Feeding and overwintering of Antarctic krill across its major habitats: the role of sea ice cover, water depth, and phytoplankton abundance. *Limnology and Oceanography*, *59*(1), 17–36.

62. Abehsera, S., Glazer, L., Tynyakov, J., Plaschkes, I., Chalifa-Caspi, V., Khalaila, I., … Sagi, A. (2015). Binary gene expression patterning of the molt cycle: the case of chitin metabolism. *PLoS ONE*, *10*(4), e0122602.

63. Clarke, A. (1984). Lipid content and composition of Antarctic krill, *Euphausia superba* Dana. *Journal of Crustacean Biology*, *4*(1), 285–294.

64. Anheller, J.E., Hellgren, L., Karlstam, B., & Vincent, J. (1989). Biochemical and biological profile of a new enzyme preparation from Antarctic krill (*E. superba*) suitable for debridement of ulcerative lesions. *Archives of Dermatological Research*, *281*(2), 105–110.

65. Perez-Riverol, Y., Bai, J., Bandla, C., García-Seisdedos, D., Hewapathirana, S., Kamatchinathan, S., … Vizcaíno, J.A. (2021). The PRIDE database resources in 2022: a hub for mass spectrometry-based proteomics evidences. *Nucleic Acids Research*, *50*(D1), D543–D552.

Legends to figures

FIGURE 1 Map of the Bransfield Strait (Antarctic Peninsula). I, II and III indicate the sampling stations ASMLR_W0011, ASMLR_W1414 and ASMLR_W1313 of the AMLR Expedition 2016 with the research vessel Nathaniel B. Palmer.

Accepted Article
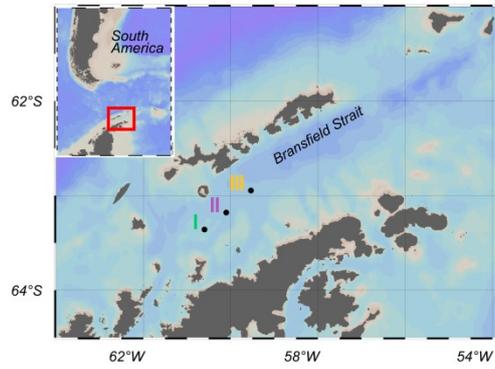
Accepted Article

FIGURE 2 Schematic workflow of krill dissection, followed by generation of transcriptome and proteome datasets based on separated body compartments (highlighted by coloring).
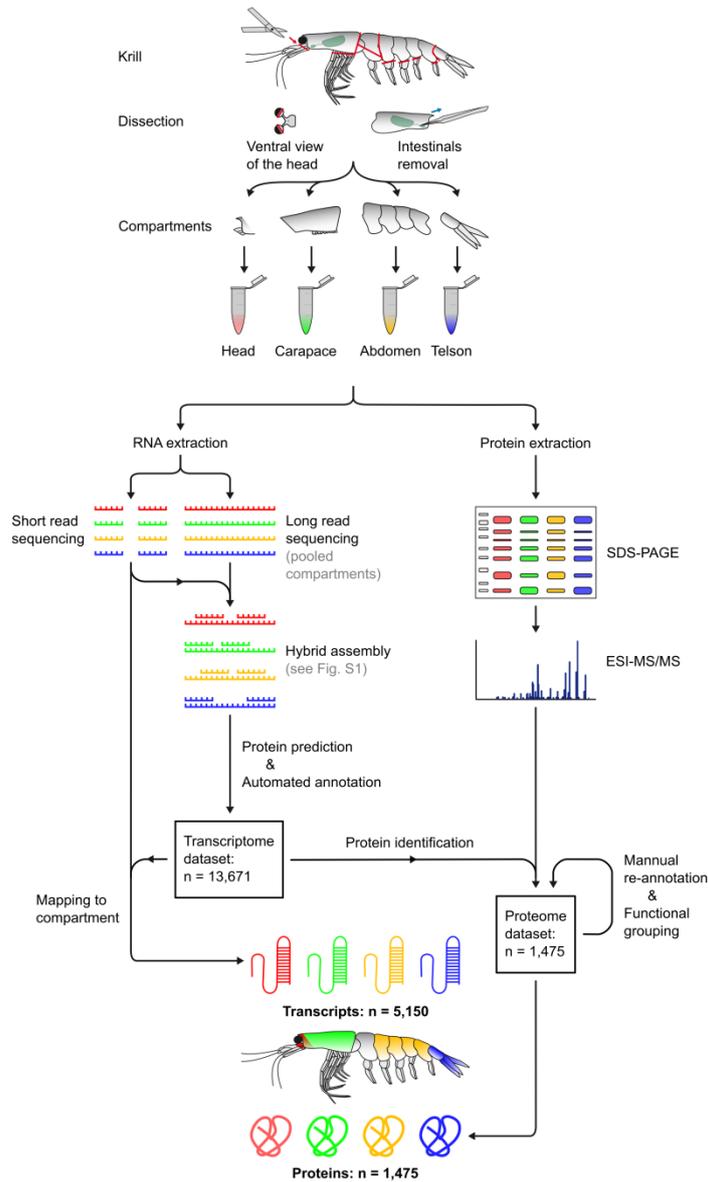
FIGURE 3 Overview of transcriptome and proteome datasets per analyzed compartment. (A) Violin plot shows density distribution of the molecular weight of identified proteins per compartment as well as of predicted proteins based on short-read *vs*. hybrid-assembled transcriptome data. The proteome datasets per compartment were generated from 15 processed krill individuals. The transcriptome dataset per compartment combines the short-read sequencing data from the four compartments of one krill individual, while the hybrid-assembled transcriptome combines long- and short-read sequences of one individual. (B) nMDS-plot of proteome datasets per krill compartment and sampling station based on the protein scores generated by nanoLC-ESI-MS/MS analyses. The grey ellipsoid areas represent 0.95 confidence, stress = 0.11. (C) Venn-diagram displaying the portions of proteins detected per individual or across compartment(s). Each ellipsoid represents data of a given compartment (pooled from 15 krill individuals). (D) Venn-diagram displaying the portions of transcripts detected per individual or across compartment(s). Each ellipsoid represents data (single measurement) of a given compartment from one krill individual.

23
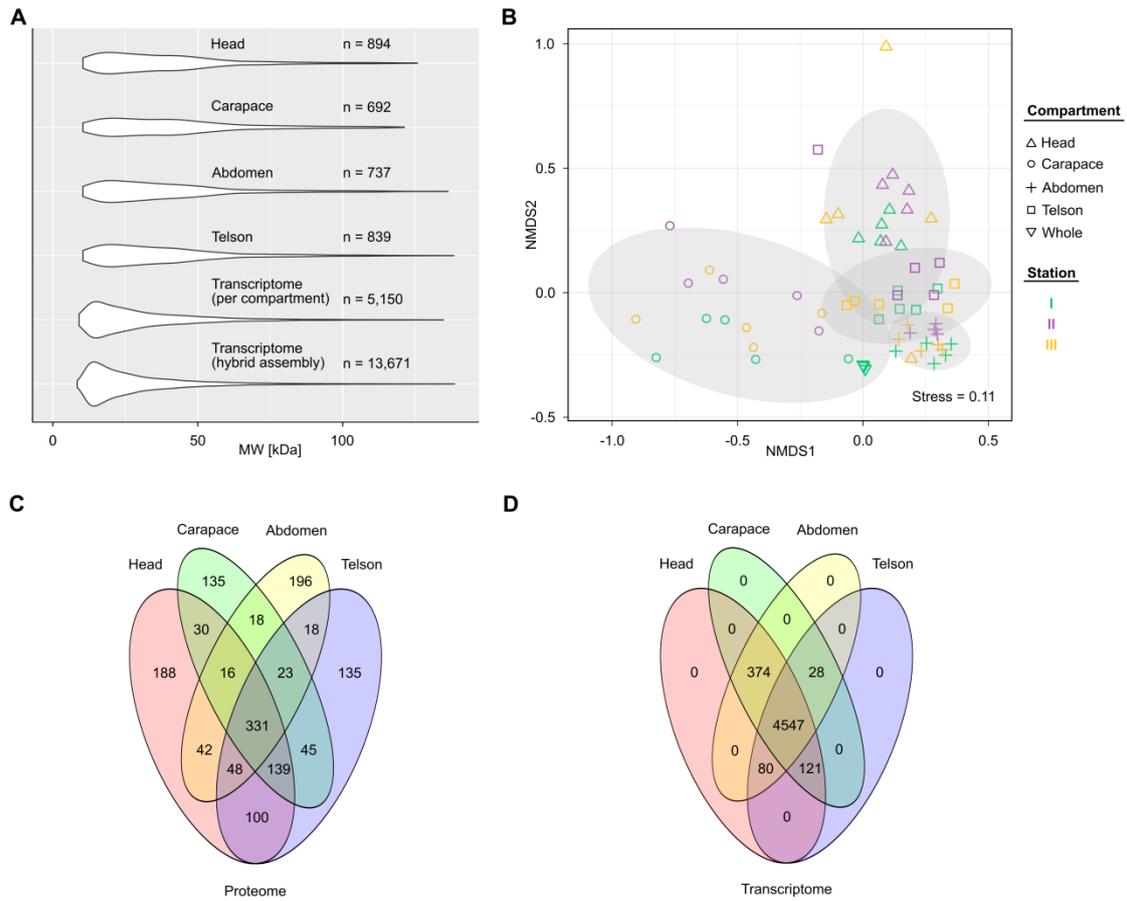
FIGURE 4 Functional grouping of proteins identified per krill compartment. The heat map represents the square root of relative abundance of different proteins of distinct function found per compartment. The relative abundance is based on the number of proteins found in each compartment.

Accepted Article
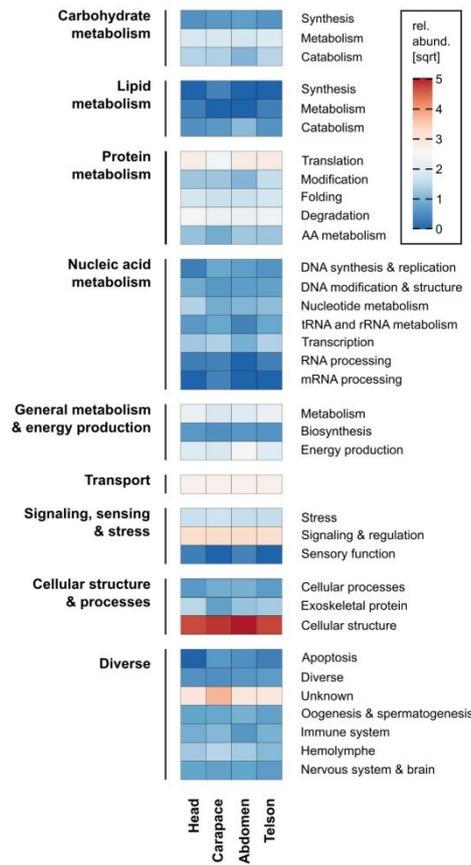
FIGURE 5 Repertoire of potential hydrolytic enzymes identified per krill compartment. The potential function as protease, CAZYme, nuclease or lipase was inferred from assignment of a given protein (predicted only or transcript and/or protein detected) to a respective GO-group, EC-number or InterPro-domain. From the 1,273 hydrolytic enzymes or CAZymes predicted from the hybrid-assembled transcriptome, 378 were detected in the transcriptomic or proteomic sub-datasets per compartment.

Accepted Article

Proteases

Proteasome

Ubiquitin proteases

Enzyme / hormone production

Immune systeme

Blood proteases

Bone proteases

Aspartic endopeptidases

Cysteine peptidases

Glutamyl peptidases

Metallopeptidases

Serine peptidases

Threonine peptidases

Acidic peptidases

Carboxypeptidases

Other peptidases

Putative peptidase functions

Head Carapace Abdomen Telson

CAZymes

Glycosyltransferases

Galactosyltransferases

Acetylgalactosaminyltransferases

Mannosyltransferases

Other transferases

Amylases

Glycosyl hydrolases

β-*N*-Acetylhexosaminidases

Glycogen metabolism

Cellulose degradation

Chitin metabolism

Chitooligosaccharide hydrolysis

Disaccharide hydrolases

Monosaccharide hydrolases

Polysaccharide deacetylases

Carbohydrate phosphorylases

Trehalose phophatases

Gluconolaconase

Lysozyme

Other CAZymes

Nucleases

Ribonucleases

Mitochondrial ribonucleases

tRNA ribonucleases

rRNA ribonucleases

Desoxyribonucleases

Ribosomal nuclease function

Transcription related nucleases

Putative (ribo)nuclease function

Lipases

Triacylglycerol hydrolases

Phospholipase

Sphingomyelin phosphodiesterases

Carboxylesterase

Lipase related

Head Carapace Abdomen Telson

Legend

Hydrolase detection in

combined transcriptomes
compartment-specific transcriptome
compartment-specific proteome
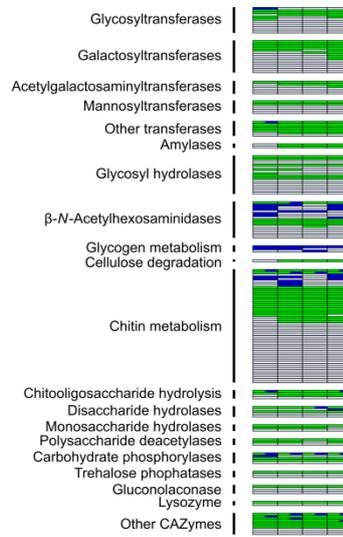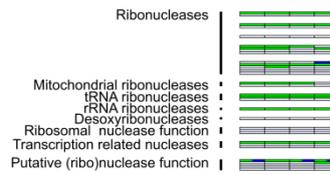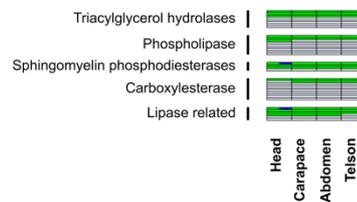
Hydrolase repertoire

	Head	Carapace	Abdomen	Telson	Σ
Proteases	45/200	26/201	26/205	34/191	250
CAZymes	16/64	13/71	7/70	17/74	99
Nucleases	1/11	0/12	0/10	2/10	14
Lipases	2/14	0/14	0/14	0/13	15
					378

TABLE 1 Hydrolases predicted from the transcriptome(T)-proteome (P) atlas of Antarctic krill assigned to potential target molecules

Target molecules	No. in T/P	Swiss-Prot entry used for functional assignment [acc. no.]
PROTEASES		
-Arg-|-Xaa-, -Lys-|-Xaa- in diverse peptides	99/5	Trypsin-1 [P00765]
-Arg^{18}-|-Thr^{19}-, -Arg^{46}-|-Gly^{47}- in coagulogen	13/2	Proclotting enzyme [P21902]
-Asn-|-Leu-, -Gly-|-Ile-, -Asn-|-Phe-, -Asp-|-Leu-, -Gln-|-Thr- in diverse matrix proteins	3/0	Matrix metalloproteinase-14 [P50281]
-Asp-Xaa-Yaa-Asp-|-Zaa (Xaa = hydrophobic) in proteins of cell apoptosis	2/0	Caspase [Q8MJC3]
-Phe-|- Arg-, -Arg-|- Arg- in diverse peptides	11/2	Cathepsin L [Q26636]
Preferentially -Arg-Arg-|-Xaa in small peptides	2/1	Cathepsin B [P07688]
-Tyr-|-Xaa-, Trp-|-Xaa-, Phe-|-Xaa-, Leu-|-Xaa- in diverse peptides	7/3	Chymotrypsin BII [P36178]
Glu-|-Xaa-, Asp-|-Xaa- in diverse peptides	2/2	Glutamyl aminopeptidase [Q32LQ0]
Phenoloxidase activating factors	21/0	Phenoloxidase-activating factor 1-3 [O97366, Q9GRW0, Q8I6K0]
-Arg^{98}-|-Ile^{99}- in proclotting factor	1/0	Clotting factor B [Q27081]
-Arg-|-Ala-, -Arg-|-Val- in Factor IX	2/0	Coagulation factor XI [Q91Y47]
-Asn-|-Xaa-, -Asp-|-Xaa- in proteins of lysosomal system	2/0	Legumain [Q9R0J8]
-Xaa - | - Asp -in diverse proteins including osteoglycin, probiglycan, collagen	2/0	Tolloid-like protein 1 / bone morphogenetic protein 1-like [A0A1S3K0K0, Q62381]
-Xaa-|-Arg, Xaa-|-Lys in diverse peptides	3/0	Carboxypeptidase M [Q80V42]
-Xaa-|-Arg-Lys-, -Arg-|-Arg-Xaa in diverse peptides	2/0	Nardilysin [Q8BHG1]
-Arg-|-Val- in Spätzle	1/0	Serine protease easter [P13582]
Gly and/or Lys linked polyubuiquinated proteins	29/4	Ubiquitin carboxyl-terminal hydrolase [P40818]
-Xaa-|-Gly-UFM1 in Ufm1-modified proteins	2/0	Ufm1-specific protease 2 [Q3B8N0]
Gly-Gly-|-Ala-Thr-Tyr; Gly-|-ε-lysine in SUMO	1/0	Sentrin-specific protease 1[Q9P0U3]

Diverse cleaving sites, proteasomen designated ubuiquinated proteins	15/14	Proteasomen α- and β-subunit [P60901, P28024]
Proteins of ERAD (endoplasmic reticulum-associated degradation)	2/0	Derlin 1 [Q9BUN8]
Diverse C-terminal AA in peptides	22/2	Carboxypeptidases A, B, E and O [Q6P8K8, P04069, P37892, P48052]
Xaa-|-Pro (-) in peptides including di- and tripeptides	1/0	Xaa-Pro aminopeptidase 1 [O54975]
Xaa-|-Yaa- in diverse peptides	9/2	Aminopeptidase N [P15144]
Xaa-|-Yaa- (Xaa ≠Arg or Lys) in diverse peptides	2/1	Putative aminopeptidase W07G4.4 [A0A6A4W0U3]
NacXaa-|-Yaa- in peptides	1/0	Putative acylamino-acid-releasing enzyme-like isoform X2 [A0A423SW39]
NacXaa -| - Yaa- (Xaa preferentially Ala, Met, Ser) in peptides	1/0	Acylamino-acid-releasing enzyme (P13676]
Xaa-Yaa-|-Zaa- (Xaa≠Ar, Lys, Yaa/Zaa≠Pro)	4/1	Dipeptidyl peptidase 1 [O97578]
Xaa-Yaa-|-Zaa- (preferentiall Yaa = Pro while Zaa≠Pro) in diverse peptides	1/0	Venom dipeptidyl peptidase 4 [B1A4F7]
Xaa-|-Yaa- (preferably Xaa=Leu) in diverse peptides	1/0	Cytosol aminopeptidase [Q5XGB9]
Xaa-|-Yaa- in diverse tripeptides and neurophil tripeptides	2/1	Leukotriene A-4 hydrolase [P09960]
-Lys-Arg-|-Xaa in neuropeptides	2/0	Neuroendocrine convertase 1,2 [P28840, G5ECN9]
Met-|-Xaa- (Xaa small uncharged AA) in diverse peptides	2/0	Methionine-Aminopeptidase [Q5ZIM5]
- -Pro-Ser-Arg-|-Xaa, Leu-Leu-Arg-|-Xaa in C3b; -Thr-Gly-Arg-|-Xaa, -Arg-Gly-Arg-|-Xaa in C4b	1/0	Complement factor I [Q61129]
Pro-|-Xaa, Ala-|-Xaa in peptides up to 30AA	2/0	Prolyl endopeptidase [P23687]
Leu-|-Xaa- in short peptides (9-16AA)	1/0	ERAP1-like C-terminal domain, aminopeptidase N-type, peptidase M1, membrane alanine aminopeptidase, N [A0A5E4N7T9]
-Glu-|-Glu in pteroylpolyglutamates	1/0	γ-Glutamyl hydrolase [Q92820]
γ-Glutamyl-binding in peptides like Glutathione	3/1	Glutathione hydrolase [Q99MZ4]
Xaa-Arg-|-Yaa, Xaa-Ala-|-Yaa in propeptide NPPA and other hormones	1/0	Atrial natriuretic peptide-converting enzyme [Q9Z319]
Diverse cleaving sites in diverse hormones including insulin	2/1	Insulin-degrading enzyme [Q9JHR7]
Xaa-Yaa-|-Zaa- in diverse peptides and	2/1	Dipeptidyl peptidase 3 [Q9VHR8]

neuropeptides (≥4AA)		
Type 1 transmembrane domains, OPA1, PINK1	1/0	Presenilins-associated rhomboid-like protein, mitochondrial [Q2KHV4]
Type 1 transmembrane domains	1/0	Protein rhomboid [P20350]
N-terminus of proteins with signal peptides for the ER	2/2	Signal peptidase complex catalytic subunit SEC11A, signal peptidase complex subunit 3 [Q9R0P6, Q6ZWQ7]
SIsopCys-|-Xaa-Yaa-Zaa in farnesylated proteins	2/0	CAAX prenyl protease 1 [O75844]
Qaa-|-Xaa-Yaa-Zaa -(Zaa≠Pro while Yaa=Glu/Asp)	2/0	Aminopeptidase NAALADL1 [Q7M758]
-Xaa-|-Yaa-(Yaa=small aliphatic) in peptides (≥5AA)	1/0	Astacin (P07584)
-Xaa-|-Yaa-, (Xaa/Yaa =hydrophobic) in neurotransmitter	8/2	Neprilysin-2 [A0A0B4K692]
-Xaa-|-Yaa- in diverse peptides	7/2	Calpain [Q11002]
Xaa-|-Yaa-Zaa, (Yaa ≠Pro and Zaa ≠ Asp/Glu) in angiotensin and oligopeptides	12/0	Angiotensin-converting enzyme [Q10714]
-Xaa-|-Yaa in diverse peptides	2/0	Lysosomal protective protein [Q3MI05]
Xaa-Yaa-Zaa-|-Qaa- in diverse peptides	2/1	Tripeptidyl-peptidase 2 [Q64560]
Diverse cleavage sites in organell proteins	4/2	Lysosomal aspartic protease [Q03168]
Unknown cleavage sites in signal peptides	1/1	Minor histocompatibility antigen H13 [Q9D8V0]
Signal peptides, Psen1, XBP1	1/0	Signal peptide peptidase-like 3 [Q9CUS9]
β-Asp-|-Xaa- in diverse peptides	1/1	Isoaspartyl peptidase / L-asparaginase [Q6GM78]
-Xaa-|-Yaa in diverse peptides	1/0	Granzyme B-like protein [A0A498NGV3]
Dipeptides, peptide bonds in general and pseudopeptides	5/3	Cytosolic non-specific dipeptidase [Q3ZC84]
Asp-|-Xaa dipeptides	1/1	α-Aspartyl dipeptidase [Q91642]
Xaa-|-Pro dipeptides	1/0	Xaa-Pro dipeptidase [P12955]
Xaa-|-Yaa dipeptides	3/0	Metallodipeptiase [A0A3R7P503]
NacXaa-|-Yaa in dipeptides including neuropeptides	5/0	N-acetylated-α-linked acidic dipeptidase 2 [Q9CZR2]
Diverse cleaving sites in short mitochondrial peptides	1/0	ATP-dependent Clp protease proteolytic subunit, mitochondrial [O88696]
-Arg-Xaa-|-Yaa in mitochondrial proteins with precurser	2/2	Mitochondrial-processing peptidase β-subunit [Q3SZ71]
-Xaa-Yaa-Zaa-|-Qaa- (Xaa=non polar,	1/0	Serine protease HTRA2, mitochondrial [B4JTT7]

aliphatic) in mitochondrial proteins		
Diverse cleavage sites in mitochondrial regulatory proteins	1/0	AFG3-like protein 2 [Q9Y4W6]
Unknown function and specificity of metallo-endopeptidases	29/1	e.g., Metalloendopeptidase [A0A423TTQ5]
Unknown function and specificity of serine-endopeptidases	84/1	e.g., Peptidase S1 domain-containing protein [A0A3R7QGW3]
Unknown function and specificity of serine-Exopeptidase	6/1	e.g., Retinoid-inducible serine carboxypeptidase [Q920A5]

CAZymes (hydrolytic)

Chitin (inner β-1,4-glycosidic bond	36/5	Chitinase 10 [Q9W5U2]
Chitooligosaccarides, *N*-acetyl-β-D-hexo-saminides (terminal β-glycosidic bond)	19/9	Chitooligosaccharidolytic β-*N*-acetylglucosaminidase [P49010]
Chitin (amid bond)	25/2	Chitin-deacetylase 1 [H9J9M0]
Diverse *O*- or *N*-acetylated polysaccharides (carboxyl or amid bond)	3/0	NodB homology domain-containing protein [A0A2J7PSN2]
GPI (Amid binding)	1/0	*N*-acetylglucosaminyl-phosphatidylinositol de-*N*-acetylase [Q9Y2B2]
Glykogen, amylose (inner α-1,4-glycosidic bond)	4/2	Glycogen phosphorylase, α-amylase [Q8HXW4, P29957]
β-1,4 or β-1,3 Glucans	1/0	Endoglucanase Z [P23659]
Malto oligosaccharide (α-1,4-glycosidic bond)	1/0	α-Glucosidase [Q9C0Y4]
Gulonolactone, galactonolactone (lactone bond)	4/0	Regucalcin [Q6TLF6]
Peptidoglycane chitodextrine (terminal β-1,4-glycosidic bond)	2/0	Lysozyme C [C1IIX1]
Lactose (β-1,4-glycosidic bond)	1/0	Lactase-phlorizin hydrolase [P09849]
Glycoproteins, glycolipids (β-glycosidic bond)	2/1	β-Galactosidase [A0A3R7MPL2]
Diverse glycans, glycoproteins (α-1,2- or α-1,3-glycosidic binding to mannose)	6/0	α-Mannosidase [C0HJB3]
Glycogen (α-1,4- and/or α 1,6-glycosidic bond)	3/3	Glycogen debranching enzyme [Q2PQH8], glycogenin-1 [P13280]
Glucosyl-acyl-sphingosine (*O*-glycosidic bond)	2/0	Glucosylceramidase [A0A6J2J528]

Glycolypids ,glycopeptides (α-1,3-glycosidic bond of *N*-acetylgalactosamine)	2/1	α-*N*-Acetylgalactosaminidase [Q90744]
Glycolypids, glycopeptides (β-1,4-glycosidic-binding of *N*-acetyl-hexosamine)	2/0	β-Hexosaminidase, α-subunit [Q641X3]
Glycoproteins (*N*-glycosidic bond between acetyl-β-D-glucosamine and Asn)	1/1	Peptide-*N*(4)-(*N*-acetyl-β-glucosaminyl)asparagine amidase [Q9FGY9]
Glycolypids, glycopeptides (α-glycosidic bond to galactose)	1/0	α-Galactosidase [A0A423SKV4]
Glycoproteins (α-1,6-glycosidic bond between fucose and *N*-acetylglucosamine)	1/1	α-L-Fucosidase [C3YWU0]
Glycoproteins (α-1,3-bond to glucose)	1/0	Neutral α-glucosidase AB [Q94502]
Nucleoside	2/0	*S*-Methyl-5'-thioadenosine phosphorylase, thymidine phosphorylase [Q7ZV22, Q99N42]
Diverse undefined α- or β-linked carbohydrate containing substrates	3/0	Putative family 31 glucosidase KIAA1161, putative mucin-17-like, β-glucuronidase [A0A5B7FTA5, A0A3R7Q3S1, A0A3R7SXU2]

NUCLEASES

DNA	2/0	40S ribosomal protein S3 [P62909]
DNA and RNA	3/1	Exonuclease 3'-5' domain-containing protein 2 [Q9NVH0], Flap endonuclease 1 [A7RRJ0], 3'-5' ssDNA/RNA exonuclease TatD [B2VG45]
dsRNA	1/0	39S ribosomal protein L44 [A0A3R7NDS2]
pre tRNA	3/0	Ribonuclease Z and P [A0A7J7ADJ6, Q0II25]
pre mRNA	2/0	Putative cleavage and polyadenylation specificity factor 73 [A0A3R7M7S7]
mRNA and miRNA	2/0	5'-3' exoribonuclease 2 homolog [Q9VM71]
mRNA	3/0	Poly(A)-specific ribonuclease [A0A7M7PY69], 5'-3' exoribonuclease 1 [Q8IZH2]
Diverse RNA types	3/0	e.g., Putative DIS3-like exonuclease 2 isoform X2 [A0A423S9D1], Exosome complex exonuclease RRP44 [Q9Y2L1], Argonaute RISC catalytic component 2 [W5MM45]
Mitochondrial RNA	2/0	Oligoribonuclease, mitochondrial [A2VE52], Mitochondrial ribonuclease P catalytic subunit [Q8JZY4]
RNA (general)	11/1	e.g., endoribonuclease CG2145 [Q9VZ49]

LIPASES

Triacylglycerol	8/0	Pancreatic triacylglycerol lipase [Q64425]
Sphingomyelin	4/1	Sphingomyelin phosphodiesterase [Q04519]
1 / 1,2-Diacyl-glycero-3-phosphocholine	6/0	Phospholipase A2 / 1-alkyl-2-acetylglycerophosphocholine esterase [P43434 / P70683]
Glycerol 3-phosphocholine	2/0	Glycerophosphocholine phosphodiesterase [Q80VJ4]
diverse carboxylesters	11/0	Esterase E4 [P35501]
1,2-Diacyl-glycero-3-phospho-(1D-myo-inositol-4,5-bisphosphate)	2/0	1-Phosphatidylinositol 4,5-bisphosphate phosphodiesterase [P13217]
Diverse phospholipids (& carboxylesters)	3/0	E.g. putative phospholipase B-like 2 [Q4QQW8]
Unknown	1/0	Dual specificity protein phosphatase 13 isoform B [Q9QYJ7]

Accepted Article